EIGHTH EUROPEAN ROTORCRAFT AND POWERED LIFT AIRCRAFT FORUM

Paper No. 2.6

CALCULATION OF ROTOR/AIRFRAME INTERFERENCE FOR REALISTIC CONFIGURATIONS

David R. Clark
and
Brian Maskew

Analytical Methods, Inc.
P.O. Box 3786
Bellevue, Washington 98009
U.S.A.

August 31 - September 3, 1982

Aix-en-Provence,
France

Abstract

The results of a fully coupled calculation of the flow around representative helicopter configurations are presented. The effect of fuselage components on the rotor flowfield and the overall wake structure is detailed and the aerodynamic interference between the different parts of the aircraft is discussed. In particular, the flowfield developed by the rotor head is followed and the effect of a rotor head cap and pylon modifications in redirecting the rotor head flow are illustrated. Good correlation between measured and calculated fuselage airloads in low-speed flight is achieved and correspondence with observed flowfield behavior is demonstrated.

INTRODUCTION

As helicopter designers work towards the development of a vehicle which can compete with fixed-wing aircraft, if not in terms of speed, at least in terms of passenger acceptance in the areas of ride quality, vibration, and noise, they are being forced more and more to acknowledge the complex interaction that takes place between the rotor and the airframe. Body/rotor interference manifests itself throughout the operational range of the helicopter; it is as significant at low speed in the form of rotor induced fuselage downloads as it is at high speed where the most important effects are the irregularities in rotor loads induced by the passage of the blades through the fuselage flowfield. Added to these effects is the controlling role of the main rotor wake in the handling qualities, passing as it does over and around the horizontal and vertical tail surfaces and the tail rotor as speed and flight conditions change. The term "interactional aerodynamics", coined by Sheriden and Smith[1], aptly describes the very involved process which controls helicopter loads, dynamics, handling qualities and performance.

Throughout the first three decades of the helicopters existence as a practical machine, the profound effect that the presence of the fuselage can have on rotor behavior was hardly acknowledged. This was largely due to the fact that there was not a strong, driving requirement to understand the interaction and rotors were designed, analysed and tested in isolation. The fact that when installed they behaved differently, trimmed at different cyclic pitch settings and had considerably different aeroelastic response and dynamic characteristics was correctly attributed, in most cases, to the presence of the fuselage. However, no serious attempt was made to understand the phenomenon and since the modest performance and dynamics goals of the period were being met, there was no incentive to refine the design methods.

The situation changed dramatically in the early seventies as a result of the competition to provide the U.S. Army with new

utility transport and attack helicopters. A prime requirement in both programs was that the designs must all be airtransportable within certain very clearly defined limits and this resulted in designs in which the rotor was placed, initially, very close to the fuselage in an attempt to reduce the overall height of the vehicle. All of the vehicles tested in this configuration exhibited undesirable dynamic characteristics which were attributed to fuselage induced rotor inflow variations.

The phenomenon was first explored analytically by Landgrebe et al.,[2] in a paper which examined the mathematical tools available for the design of the new generation of rotor craft. In this work the flowfield induced by the fuselage in the region of the rotor was calculated by an early potential flow configuration modelling program. For this early study there was no direct coupling of rotor and fuselage effects, and the velocities calculated in the rotor plane by the fuselage analysis were simply fed as inflow into the rotor analysis. Because of the size of the individual programs and the limitations of the computing facilities available at the time, no coupling of the rotor on fuselage effects was attempted beyond very simple source plane or vortex tube rotor models. Despite these limitations the analysis was used with some success to explore alternative rotor locations. The study showed how, when operating close to the fuselage, the rotor is exposed to an azimuthally varying inflow, predominantly up over the nose and down aft of the shaft but containing higher harmonics, which significantly degrade the aircraft vibration environment. Also it was realized that the upwash over the front fuselage was severe enough, causing very large increases in angle of attack as the blade passed through the forward portion, to precipitate stall as far out as mid-span. Inclusion of the fuselage induced flowfield in the dynamic analysis dramatically improved correlation with measured data.

Fuselage/rotor interference has been explored from both experimental and analytical sides. Noteworthy from the experimental point of view has been the work of the group at NASA Langley. Following the early work of Wilson and Mineck,[3] directed mainly at handling qualities and low speed fuselage loads, the work of Freeman with Mineck,[4] and later with Wilson[5] explored systematically the influence of body shape and relative rotor/body position on fuselage and rotor airloads. They showed how with increased fuselage width and reduced body/rotor spacing the performance of both systems is degraded. The work of Sheriden and Smith,[1] concentrating on a particular configuration also explored the effects of body/rotor placement. More recently, Betzina and Shinoda[6] working with a scale model of a wind tunnel test module (from the NASA Ames 40 x 80 wind tunnel) have examined coupled rotor/body integrated performance. Formerly a rarity, tests of rotor/fuselage combinations are now standard procedure as designers try to define more closely the differences

between analysis and actuality and between model and full-scale test results. Reference 6 presents a fairly typical outline of the gaps that still exist in the understanding of the coupled flowfield.

In parallel with the expansion of the experimental data base, work has continued on the development of analytical tools to explore rotor/body phenomena. Several different approaches to modelling the flowfield have been employed ranging from involved combinations of vortex filament wake models and full fuselage panel models to simple stacked vortex ring arrays. In all cases, however, inclusion of the effect of the presence of the fuselage in the description of the rotor inflow improves the prediction of unsteady effects.

At a rotor wake workshop held by the U.S. Army Research Office (AROD), Smith[8] presented a method where the fuselage was represented by a single source element in a uniform flow and the rotor by a series of constant strength vortex rings, displaced upwards as they passed through the sphere of influence of the body source. Despite the relative crudity of the model, the predicted rotor loading shape was good. The same basic model was used by Young.[9] With a more refined fuselage model and considering both vertical and horizontal displacement of the vortex rings, he was able to show some improvements in correlation with test data. Incorporation of cyclically varying circulation around the rings further enhanced the correlation.

A more detailed analysis which more accurately represents the fuselage with a complex panel model and the rotor with a wake filament model was used by Landgrebe et al.[1] The method was used in the work discussed in Reference 7 and in Reference 10. Here, the flow around the panel model is first calculated and the velocity field in the plane of the rotor determined. This is used as input to a rotor performance calculation which can include as much detail as desired, up to and including a full filament wake distortion calculation. It is not clear from the published work whether any higher-order coupling is involved. Certainly, in the schematics presented in Reference 7, the arrows connecting fuselage and rotor aerodynamics modules only go one way, from fuselage to rotor, implying no higher-order coupling than a simple rotor onset flow modification. Comparison between results predicted using the method and test data show good agreement.

A similar approach is taken by Huber and Polz.[11] Using a detailed panel model they calculate the flow in the plane of the rotor for input to a rotor analysis. Again, no higher-order coupling is used. This is reflected in the fuselage induced upwash profiles presented in Reference 11, which are symmetric about the center plane. If coupling had been present, the upwash contours would have been asymmetric, reflecting the differences in loading between the advancing and retreating inboard blade sections. Despite this, they show very graphically the large

impact of the fuselage on the rotor loads, especially in the region of the fourth and fifth harmonic.

Huber and Polzl[11] also present results from earlier studies where, for the first time, attempts have been made to calculate the effect of regions of separated flow on downstream components. The earlier work,[12] presents the method in detail. Following the by now conventional technique (see References 13 and 14), the authors, using a panel method and streamline procedures, calculate the extent of regions of separated flow; then, with a novel volumetric vorticity singularity model, are able to determine the velocity field inside the separation zone downstream. They do not, however, present any calculation on the effect of these flows and, in fact, their sample cases are un-naturally truncated. This is done since the type of singularity model used in the analysis cannot handle a direct vortex/surface intersection.

Another theoretical approach to the body/rotor problem is that taken by Freeman.[15] Again, using a basic panel model for the fuselage and a vortex tube model of the rotor wake, following Heyson,[16] he was able to show quite impressive correlation between the results of his analysis and body/rotor test data. However, there was no coupling present between rotor and fuselage flows, the rotor model being simply used to perturb the fuselage model onset flow, and, although the rotor wake was contracted, no fuselage induced wake distortion was introduced.

None of the rotor/fuselage analyses examined couples fully the flowfields of the two components to the extent that terms of higher than first order; that is, fuselage on rotor (References 2, 7 and 9) or rotor on fuselage (Reference 15) are included, and none have been able to calculate the deformation of the rotor wake in the presence of the fuselage or handle the direct vortex wake/fuselage cutting situations. The reasons for this were outlined by the present authors at the U.S. Army Conference on Wake Modelling in 1979, Reference 17, and in detail in Reference 18. The lack of an adequate coupling analysis results partly from the limited capacity of the computing machines then in use (the fuselage panel codes and vortex wake codes on their own consuming most of the machine capacity--precluding directly coupled calculation), but mostly from the inability of the potential flow models to handle the close approach of strong singularities in the external flow and direct vortex/surface encounters.

The goal of the present study was a full description of the highly interactive helicopter flow field including powerplant exhaust, horizontal and vertical stabilisers, tail or other auxiliary rotors and separated wakes from upstream components such as bluff rotor heads. This was made possible by the coupling of a rotor module to an advanced potential flow modelling code. The program, designated VSAERO (Vortex Separation AEROdynamics), References 19 and 20, uses combinations of doublet and source singularities, together with changes in the way in which the boundary conditions are applied, to solve for the local, scalar

doublet strength. This is differentiated to define the local velocity field. Techniques have been developed to handle not only close vortex approach but also direct wake cutting. The rotor wake (wakes if more than one rotor is present) is represented by time-averaged vortex sheaths which are allowed to deform in the presence of the fuselage flowfield. The rotor/fuselage coupling is made through a blade element model for the rotor supplied with inflows from the fuselage/wake calculation and feeding back circulation strengths to the wake.

The model has been used with some success to look at basic body/rotor performance over an advance ratio range from 0.05 to 0.3. Correlation of fuselage loads inside the wake interference zone is good. The test data used for the correlation was that of Freeman and Mineck.[4] The same basic configuration was used as a starting point for a study of the effects of adding configuration components and a full build-up was carried out. The effects of adding horizontal and vertical stabilizer, tail rotor, engine nacelles and exhaust plumes, a rotor head representation, and finally, a rotor head fairing were explored. The role of the rotor head "beanie" and pylon modifications in deflecting the center portion of the rotor wake downwards was demonstrated.

DESCRIPTION OF THE ANALYSIS

The basic procedure used for the determination of the combined body/rotor flowfield remains very much as was originally outlined in Reference 17. The solution proceeds iteratively as shown in Figure 1. Basic input consists of the fuselage geometry, the rotor parameters and an initially prescribed wake shape. The first step is the calculation of the rotor loads at the input flight condition. At this stage, uniform inflow is assumed. With rotor loading determined as a function of radius and azimuth, this is passed over to the body aerodynamics calculation to set the boundary conditions for the panel model of the rotor disc and to feed the vortex sheath wake attached around the edge of the disc.

The solution then passes to the body aerodynamics calculation, solving for the unknown body singularity strengths. With these known, the initially prescribed rotor wake is relaxed and allowed to take up a force-free position in the flowfield around the body. With the wake in its new position, and with the body influence in the plane of the rotor determined, the rotor onset flow is recalculated. The solution is then returned to the rotor blade element calculation and the next iteration proceeds. At moderate and high advance ratio, $\mu > 0.1$, experience has shown that only two body/rotor/wake iterations were required to converge the solution. At $\mu = 0.05$, a maximum of four iterations have been required.

Body Aerodynamics

The aerodynamics of the body and wake components are calculated using program VSAERO. Program VSAERO (Vortex Separation AEROdynamics analysis) is a refined surface singularity analysis which removes the limitations of the earlier generations of codes (Reference 21 is typical) and provides a much more rigorous aerodynamic model without sacrificing the simple, flat panel model of the aircraft shape. The program development was funded by NASA and the U.S. Navy and has been documented most recently in Reference 20. Using a combination of source and doublet singularities and modifying the way in which the boundary conditions are applied, the program solves for the local doublet strength. This is then differentiated to obtain the local velocities. The method of solution has been extended to handle strong external vortex/surface interactions and is no longer constrained as were the earlier codes to align external flow vortices along panel edges. This permits relaxation of the wake (iteration to a force-free location) without the repanelling between iterations that was implicit in the earlier programs.

The program used in the present study was the potential flow model for general configurations with multiple components. The program capacity is for 1,000 panels on each side of the plane of symmetry with an additional 1,000 panels of separated wake. The wakes may be shed by all the components along any edge (say the wing tip edge) and any or all wake(s) may be relaxed. Engine inlet and exhaust flow may be modelled and high energy jets simulated. The program can also be used to survey the velocity field off the body. Also available but not used in this study are on- and off-body streamline capability, coupled viscous/potential flow iterations with extensive separation modelling and time-stepping and harmonic wake analysis, respectively, for large and small amplitude unsteady body motions.

The principal problem working against the application of the old panel codes to the rotor and other highly interactive flows is their inability to handle wake/surface cutting. In a conventional source or vortex-lattice method, impact of a vortex element on the surface anywhere other than along a panel joint will cause a divergent solution. In VSAERO, because of the nature of the solution, it simply causes a jump in the doublet distribution along the line of the cut. Provided that this jump is accommodated in the surface differentiation used to determine the velocity field, the resulting solution can be continuous through the cut. To demonstrate the procedure on a configuration somewhat simpler than the typical helicopter, a simple test case was set up.

The Wake Cutting Procedure

In order to explore whether the potential jump associated with wake cutting would violate the basic formulation or at least cause a numerical problem in the solution, a test case was set up with a vertical surface ahead of a wing, Figure 2. The vertical surface is modelled with a 3 x 12 panel array on a zero thickness lifting surface. The tips of this surface have a 5 degrees backward rake. The vertical surface is set at 20 degrees to the x-axis; i.e., to carry a side force directed to the plane of symmetry. The horizontal wing has a rectangular planform with an aspect ratio 4 and a NACA 0012 section: it is modelled with a 24 x 20 array of panels on the main surface and a 3 x 12 array on the half-round tip. The spanwise panelling is arranged with concentrations near the tip and just outboard of the spanwise station of the vertical surface trailing edge (i.e., where the maximum vortex wake interaction is expected to occur). The onset flow was set at 10 degrees.

Figure 3 shows two views of the calculated wake geometry after three wake shape iterations. The side view, Figure 3(a), demonstrates a very nice behavior of the basic vortex roll-up calculation on the vertical wake. The top view of the wake geometry (Figure 3(b)) shows reasonably good behavior except that beyond the wing trailing edge there are some local problems due to the widening of grid planes used in the wake calculation.

A spanwise cut through the doublet distribution, Figure 4, shows the expected jump in doublet value (i.e., jump in surface perturbation potential) due to the vertical wake intersection. The jump occurs at slightly different spanwise locations on the upper and flower surfaces due to the local tilt of the wake panels at this station (x/c = .25). It is easily verified that the spanwise doublet gradient (i.e., Vy), plotted in Figure 5, is essentially continuous as we pass through the wake--only the doublet value is discontinuous. At this time the code has no way of knowing about this particular jump in value and so it would take gradients across the cut, whereas it should "step back" from the cut when evaluating local doublet gradients. Similar good behavior was also noted in the other velocity components and in the surface pressure distributions. The vortex pair from the vertical surface clearly dominates the spanwise flow on the wing. The otherwise inboard flow (negative Vy) on the wing upper surface has been totally reversed by the vortices except in the very tip region where there is clearly still some flow moving around from the lower to the upper side.

Rotor Aerodynamics

Rotor aerodynamics is calculated using a simple blade element theory model. Inflow velocity, after the first iteration during which the inflow is assumed constant at the momentum value, is calculated in the body/wake portions of the program and passed over to the rotor internally. Only rigid

blade flapping is permitted. No aeroelastic effects are considered. The rotor module has deliberately been isolated from the rest of the calculation so that, if required at a later time, a more involved rotor algorithm may be substituted. The present module may be operated at prescribed collective and cyclic pitch settings or may be allowed to iterate to requested gross weight and rolling and pitching moment targets.

The Computer Program

The Body-Rotor analysis program (BodRot) is a simple extension of the basic program VSAERO. The rotor program is a self contained subroutine called by the main program whenever a type-4 patch, a rotor or propeller disc, is loaded. The code is available as an update deck to the basic program. The analysis has been loaded and executed on Control Data Cyber 176 and 7600 machines and has recently been demonstrated on CRAY. The only additional data required beyond the general configuration description is the rotor details and the blade section airfoil data.

DISCUSSION OF RESULTS

Basic Body/Rotor Results

The model chosen for the study was that tested by Freeman and Mineck[4] scaled to a rotor radius of 20 feet. This size was chosen to give a full scale machine typical of helicopters in the small to medium size range. A target vehicle weight of 7,000 lb. gave a rotor thrust coefficient of 0.00554. Calculations were made at three advance ratios: these were 0.05, 0.15 and 0.3. The two low values were chosen to provide an overlap with the Freeman data, the high value to give a more realistic case for studying body rotor interference close to the cruise condition.

Figure 6 shows an oblique view of the basic panel model of the fuselage and rotor. Correlation with measured surface pressure data is generally acceptable. Certainly on those regions most influenced by the rotor wake, the fuselage aft of the rotor center, agreement is good. Figure 7 shows comparisons at station 17.6 for the two advance ratios. The comparison is presented at the same scales as it was presented in the original report,[4] at the $\mu = 0.15$ advance ratio. Correlation over the front fuselage, Figure 8, is less good. This probably results, to a certain extent, from the relative crudity of the panel model in this region, and from a mismatch in the calculated and measured angles of attack. Wind tunnel corrections had been allowed for the test data. The lower surface was made deliberately sparse to allow for increased panel density on the upper and aft sections. Sections within the rotor influence could be less sensitive to model rigging angle/analysis angle mismatch than would be those sections on the nose.

An oblique view of the low advance ratio case, Figure 9, shows the wake draped over the fuselage. This is explored further in Figure 10 where cross sections are taken through the wake as it develops aft and downwards. It is interesting to note the roll-up of the edges of the rotor wake. Since the wake is made up of rectilinear vortex elements, some crossing is to be expected in the model. In practice, however, the wake simply coils around itself. In the model, the wake leaving the leading edge of the disc moves first upwards as it is convected aft. It then passes downward, held up above the isolated rotor position by the flow developing around the fuselage. The wake cuts the pylon, recombining above the tail cone in the region aft of the rotor head. In the absence of detailed experimental data on wake/body cutting, it is difficult to judge how valid the present model is in this region. It does, however, appear to behave as a membrane made of discrete, traverse vortex elements would act on an oblique approach to a surface, first deforming as the surface is sensed and then, at some point, dividing with the torn edges rolling up along the surface. The theoretical wake does not, of course, tear. Here, the streamwise elements defining the edges of the wake panels pass, following the external flow lines, over the body, reacting to their reflections in the surface while the cross elements pass through the surface connecting to the adjacent streamwise filament. These carry with them, into the body solution, the jump in doublet strength which accounts for the change in flow conditions from outside to inside the wake.

The effectiveness of the procedure for handling the wake cutting problem is shown in Figure 11(a) where the doublet distribution along the pylon waterline cut is shown. The jump in strength across the wake edge is clear. In Figure 11(b), the velocity component in the streamwise direction shows no perturbation other than the changes in velocity associated with the changes in shape.

Based simply on the relative magnitude of the rotor inflow velocities, the effect of the rotor on the fuselge would be expected to decrease with increasing flight speed. This shows very clearly in Figure 12 where the vertical velocity component along a horizontal cut close to the model maximum is plotted for values of advance ratio of 0.05 and 0.15. In both cases the fuselage was set at the same angle of attack and the rotor was trimmed for level flight at 7000 lb. GW and 12 $ft.^2$ of drag with nominally zero pitching and rolling moment. At $\mu = 0.15$, the rotor-induced vertical velocity is very small and differences between right and left (advancing and retreating) sides are slight. At $\mu = 0.05$, however, where the rotor downwash is a substantial fraction of the forward flight speed, the side to side differences are quite marked with the more highly loaded, inboard, advancing side showing the stronger effect.

The trend of the influence of the fuselage on the rotor with speed is, of course, reversed as it is stronger at higher speeds. This is best illustrated by comparing the blade angle of attack

distribution at an inboard and outboard station (0.4 and 0.9 R/R_{TIP}) for advance ratios of 0.05 and 0.30 shown in Figures 13 and 14. As expected, the strong upwash over the nose and downwash over the aft fuselage are reflected in regions of increased and decreased angle of attack. At $\mu = 0.05$, the fuselage effect on the rotor is almost negligible; at $\mu = 0.30$, it dominates the picture. These dramatic changes in angle of attack result from the fuselage-induced flowfield. Earlier analyses, the work of Landgrebe et al.[2] and Polz[13] are typical, failing to include coupling between fuselage and rotor flowfields, produce an inflow distribution that is symmetrical. The present approaches with full coupling shows a more nonuniform upwash, Figure 15, and one which certainly, in reflecting the lateral differences in rotor loading, is not symmetrical about the fuselage centerline.

The Effect of Configuration Elements on the Rotor/Fuselage Flowfield

Adding representative horizontal and vertical stabiliser surfaces to the basic configuration has only a weak influence on the rotor flowfield, but serves as a good example of the ability of the analysis to handle calculations where fuselage elements are embedded in and, in fact, pierce wake regions.

The further addition of nacelle units, Figure 16, however, has a substantial effect on the rotor flowfield. Mounted on either side of the pylon they produce changes in the upwash field with an interesting indirect effect illustrated in Figure 17. This shows the angle of attack variations with azimuth at radial stations of 40% and 90% of the blade radius. Although mounted at 90° and 270° azimuth, their direct effect is seen all around the azimuth. However, the retreating blade change occurs in the relatively low energy region of the disc; for advance ratios higher than the 0.15 of the present example, it would be in the reverse flow region, and so the lateral rotor loading is put out of balance. The rotor must, therefore, be retrimmed and this is the indirect effect that is causing the observed changes at the outboard station.

Adding a mass in the center of the disc has an even more dramatic effect. The size of the blockage was chosen to represent the volume and frontal area of a rotor head with some kind of vibration adsorption equipment superimposed. The separated flow behind the rotor head was modelled and the wake transport and deformation was calculated in parallel with the deformation of the main rotor wake. Figure 18 shows an oblique view of the configuration and the calculated wake trajectories. The main rotor wake is present, but has been omitted from the picture for reasons of clarity. The calculated path aft and down matches the observations of many authors. It should be pointed out here that no attempt was made to model the effects of hub rotation and, consequently, any lateral displacement is the result of asymmetry in the steady flow about the fuselage and

through the rotor. Figure 19, showing cross sections through the aft fuselage and all the wake elements at the mid-span and tip of the downstream blade shows the wake convection more clearly.

The presence of the rotor head has a very strong effect on the blade behavior. Forced to accommodate not only the flow distortion associated with the presence of the rotor head mass itself, it must also pass through the "dead" region of the separated wake. The blade response to this perturbation dominates Figure 20 where the azimuthal variation of blade angle of attack at two stations is presented. Clearly, this will have a profound effect on the calculated aeroelastic response of the blade and could well be softened when elastic effects are included. The substantial changes in cyclic pitch required to retrim the rotor in the presence of the rotor head can be seen in the differences in local angle of attack at the outboard station also shown in Figure 20. It should be pointed out that this treatment of the rotor head as a simple bluff shape with no base ventilation probably is exaggerating the effect. Further study is required. Several studies, Reference 23 is typical, have shown how the rotor head wake and regions of upper body separated flow can be controlled by the addition of a rotor head cap or "beanie" or by contouring of the aft pylon to provide an edge separation which rolls up and convects the separated flow out of the region of harm. Both these devices were studied using the analysis. Figure 21 shows the panel models of rotor head cap and the aft pylon modification and their wakes. The success of both devices in depressing the disturbed flow and the center of the main rotor wake is clearly seen in the wake cross-sections at the trailing edge of the rotor disc shown in Figure 22. The strong roll-up of the wakes on the rotor cap and modified pylon shapes contrasts sharply with that noted on the basic rotor head. Again, although the main rotor wake was included in the calculation, it was omitted from the drawing for reasons of clarity. It should be noted that no strong hub wake/blade interference was found for either modification.

Full-Configuration Study

The section above has shown how the analysis can be used to explore the influences of detailed configuration changes. The analysis also has the capability to explore full vehicles, including multiple rotors. This is illustrated in Figure 23. Here, the full machine is modelled, fuselage, pylon, engine nacelles, horizontal and vertical stabiliser, rotor head cap and, finally, main and tail rotors. For the lifting components vortex sheath wakes, not shown in the drawing, are attached around the edges. The rotor head cap and the stabilisers are modelled, in the interest of economy, using a lifting surface rather than a full surface singularity model. If machine capacity had been available, a full panel model, including thickness effects, would have been used. Even with this simple model, however, the effect of the tail rotor on the vertical stabiliser in the presence of the main wake can be demonstrated. In Figure 24 the chordwise

the main wake can be demonstrated. In Figure 24 the chordwise loading with and without tail rotor is shown. The graph shows the difference in pressure coefficient between the upper and lower surface of the vertical stabiliser. No attempt has been made to trim the lateral forces on the tail rotor/fin combination and the tail rotor is simply operating at a set fixed collective. As a consequence, the vertical stabiliser is operating in an inflow field which tends to generate side force counter to that of the tail rotor. This is, of course, unproductive and in practice the two would be adjusted to complement rather than fight each other.

CONCLUSIONS AND RECOMMENDATIONS

An analysis has been developed which permits a fully coupled solution of the rotor and airframe behavior of realistic helicopters. The effect of the rotor/body coupling on the rotor inflow has been illustrated and the significance of the effect of configuration elements, particularly the rotor head and rotor head cap devices, demonstrated. The role of the rotor head cap and pylon flow control devices in moving the separated wake and the center of the main rotor wake was shown for a typical helicopter configuration.

Several additional steps must be taken to verify the usefulness of the analysis beyond the performance and handling qualities applications of the present study. In order to be useful to the dynamicist, the higher harmonics of loading associated with discrete blade vortex encounters must be added (how this can be achieved was discussed in the earlier report on this work by the present authors, Reference 18), and the resulting blade loadings coupled to an aeroelastic analysis. This would be further facilitated if the program capacity were expanded beyond the current 1000-panel version. If this were done, much greater detail in rotor disc modelling would be possible than is possible with the present, relatively crude, 32 azimuthal steps in the rotor solution.

Despite the relative crudity of the model, the authors feel that with this analysis it is now possible to explore the highly interactive flowfield around the helicopter and that other configurations previously analysed with relatively empirical approaches can now be studied in detail with a representative model. The most likely candidate in this category is the tilt-rotor concept, where now, with the demonstrated wake cutting capability of the present program, a full analysis of the dual rotor, wing, fuselage flowfield becomes possible.

ACKNOWLEDGEMENTS

The authors would like to acknowledge the contributions of their colleagues at Analytical Methods, Inc. The body/rotor work

was carried out in part under NASA Contract NAS2-10620. The development of the basic VSAERO program was carried out under NASA Contract NAS2-8788. Both contracts were administered through the NASA Ames Research Center, Moffett Field, California.

REFERENCES

1. Sheridan, P.F. and Smith, R.P., "Interactional Aerodynamics--A New Challenge to Helicopter Technology", Presented at the 35th Annual Forum of the AHS, 1979.

2. Landgrebe, A.J., Moffit, R.C. and Clark, D.R., "Aerodynamic Technology for Advanced Rotorcraft", Paper Presented at the AHS Symposium, Essington, PA, 1976.

3. Wilson, J.C. and Mineck, R.E., "Wind Tunnel Investigation of Helicopter-Rotor Wake Effects on Three Helicopter Fuselage Models", NASA TMX-3185, 1975.

4. Freeman, C.E. and Mineck, R.E., "Fuselage Surface Pressure Measurements of a Helicopter Wind Tunnel Model with a 3.15-Meter Diameter Single Rotor", NASA TM-80051, 1979.

5. Freeman, C.E. and Wilson, J.C., "Rotor-Body Interference (ROBIN) Analysis and Test", Paper Presented ast the 36th Annual National Fourm, AHS, Washington, D.C., May 1980.

6. Betzina, M.D. and Shinoda, P., "Aerodynamic Interaction between a 1/6-Scale Helicopter Rotor and a Body of Revolution", NASA TM-84247, Ames Research Center, Moffett Field, CA, June 1982.

7. Arcidiancano, P.J. and Sopher, R., "A Review of Rotor Loads Prediction Methods", AGARD Conference Preprint AGARD-CP-334-14, Fluid Dynamics Specialists Meeting, London, May 1982.

8. Smith, R.V., "Some Effects of Wake Distortion due to a Fuselage Flowfield on Rotor Thrust Limits", Paper Presented at ARO Workshop on Rotor Wake Technology, Raleigh, N.C., 1979.

9. Young, C., "Development of the Vortex Ring Model and its Influence on the Prdiction of Rotor Loads", AGARD Conference Preprint, AGARD-CPP-334-11, Fluid Dynamics Specialists Meeting, London, May 1982.

10. Jepson, D., Moffitt, R., Hilzinger, K. and Bissell, J., "Analysis and Correlation of Test Data from an Advanced Technology Rotor System", NASA CR-152366, July 1980.

11. Huber, H. and Polz, G., "Studies of Blade to Blade and Rotor-Fuselage-Tail Interferences", AGARD Conference Reprint,

May 1982.

12. Stricker, R. and Polz, G., "Calculation of the Viscous Flow Around Helicopter Bodies", Paper Presented at the 3rd European Rotorcraft and Powered Lift Forum, Aix-en-Provence, France, September 1977.

13. Clark, D.R., Dvorak, F.A. et al., "Helicopter Flow Field Analysis", Final Report for Period April 1977 - September 1978, USARTL-RT-79-4, Ft. Eustis, VA, 1979.

14. Clark, D.R., "A Study of the Effect of Aft Fuselage Shape on Helicopter Drag", Paper Presented at the 6th European Rotorcraft and Powered Lift Aircraft Forum, Bristol, England, September 1980.

15. Freeman, C.E., "Development and Validation of a Combined Rotor-Fuselage Induced Flowfield Computational Method", NASA TP-1656, 1980.

17. Clark, D.R., "An Outline of a Method for Predicting Fully Coupled Body/Rotor Interference", Paper Presented at the ARO Workshop on Rotor Wake Technology", Raleigh, N.C., 1979.

18. Clark, D.R. and Maskew, B., "An Analysis of Airframe/Rotor Interference in Forward Flight", Paper Presented to the 7th European Rotorcraft Powered Lift Aircraft Forum, Garmisch-Partenkirchen, FRG, September 1981.

19. Maskew, B. and Dvorak, F.A., "Analysis of Vortex/Surface Interactions Using Panel Methods", Paper Presented at the 1981 U.S. Air Force - FRG DEA Meeting, Gottingen, West Germany, April 1981.

20. Maskew, B., "Prediction of Subsonic Aerodynamic Characteristics--A Case for Low-Order Panel Methods", AIAA J. Aircraft, Vol. 19, No. 2, February 1982.

21. Hess, J.L. and Smith, A.M.O., "Calculation of Potential Flow about Arbitrary Bodies", Progress in Aeronautical Sciences, Vol. 8, Pergamon Press, 1967.

22. Maskew, B. and Rao, B.M., "Calculation of Vortex Flows on Complex Configurations", Paper to be Presented to the Joint ICAS/AIAA Conference, Seattle, WA, August 1982.

23. Roesch, P. and Vuillet, A., "New Designs for Improved Aerodynamic Stability on Recent Aerospatiale Helicopters", Paper Presented at the 37th Annual Forum of the AHS, New Orleans, LA, 1981.

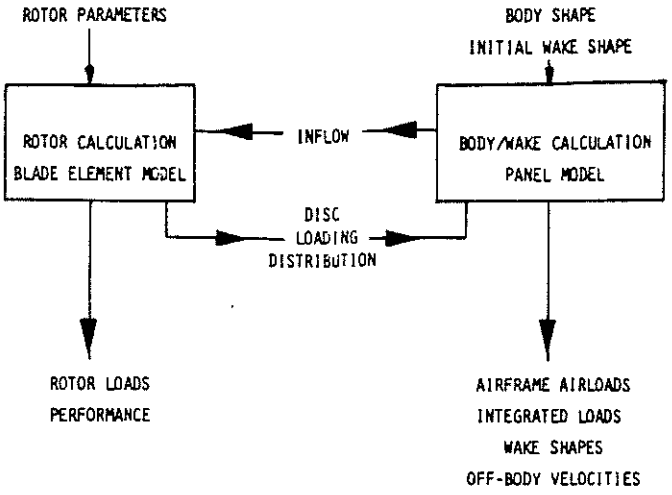

Fig. 1. Body/Rotor Interference Calculation Schematic.

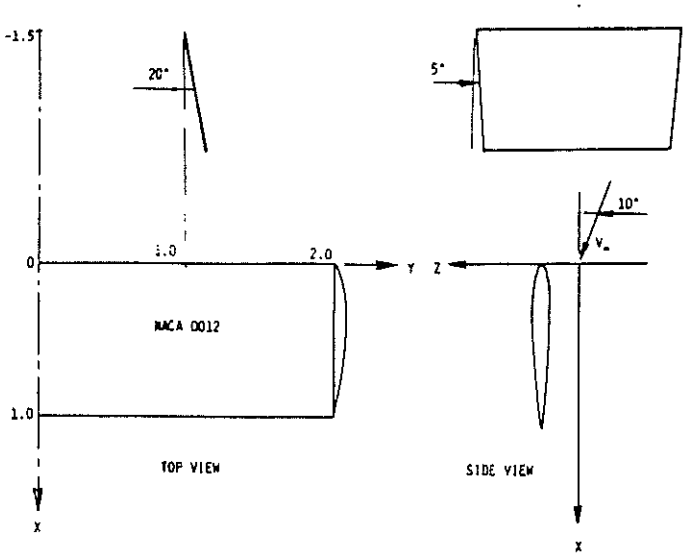

Fig. 2. Schematic of Wake Cutting Model.

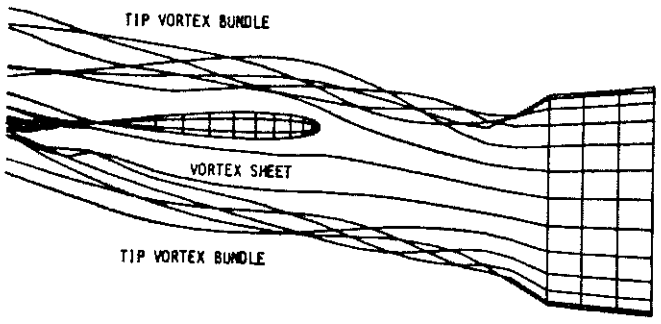

(a) Side View

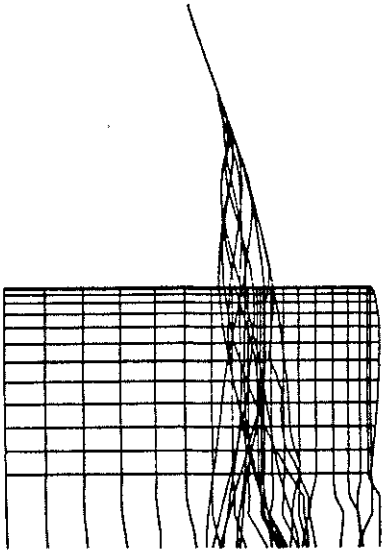

(b) Top View

Fig. 3. Wake Cutting Study.

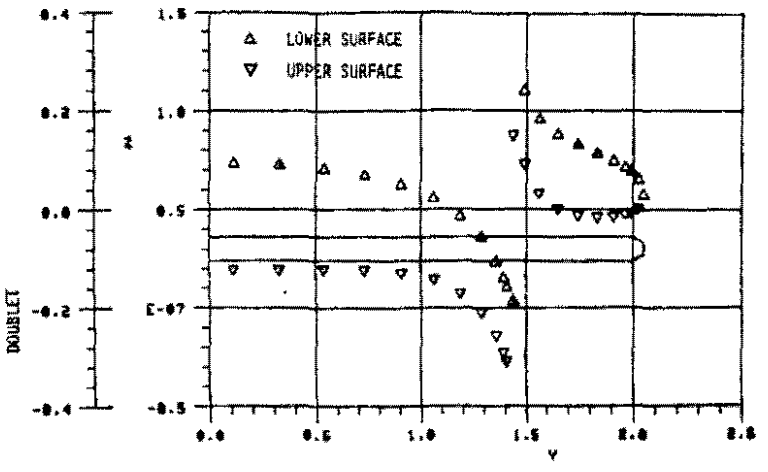

Fig. 4. Wake Cutting Study--Spanwise Doublet Distribution (0.25 Chord).

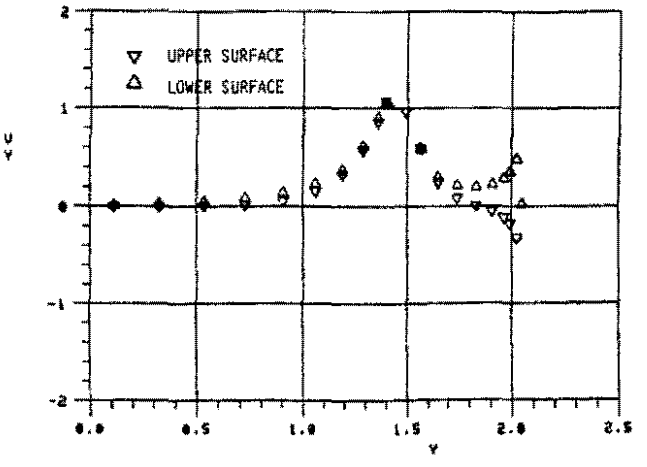

Fig. 5. Wake Cutting Study--Spanwise Velocity (0.25 Chord).

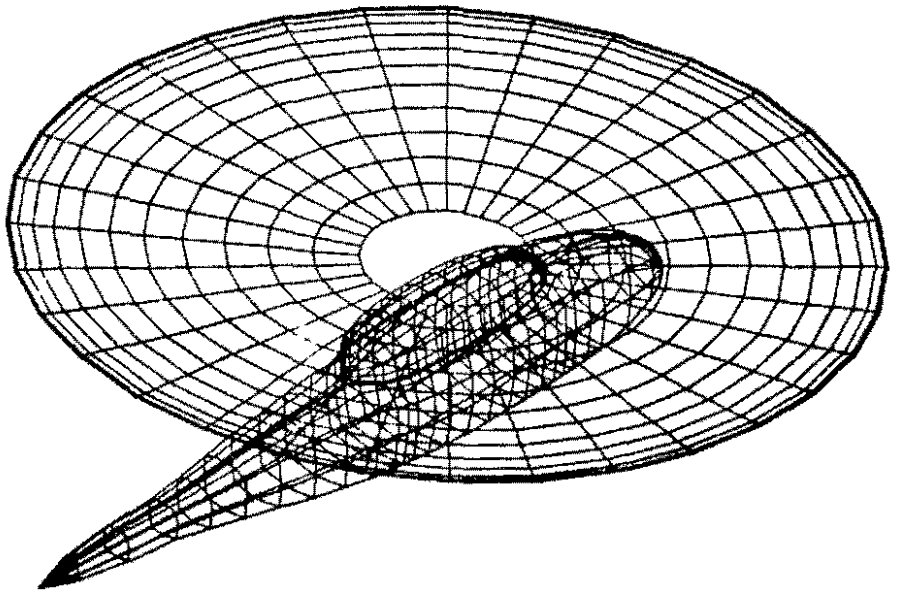

Fig. 6. Basic Panel Model for Body/Rotor Studies (After Freeman and Mineck, Ref. 4).

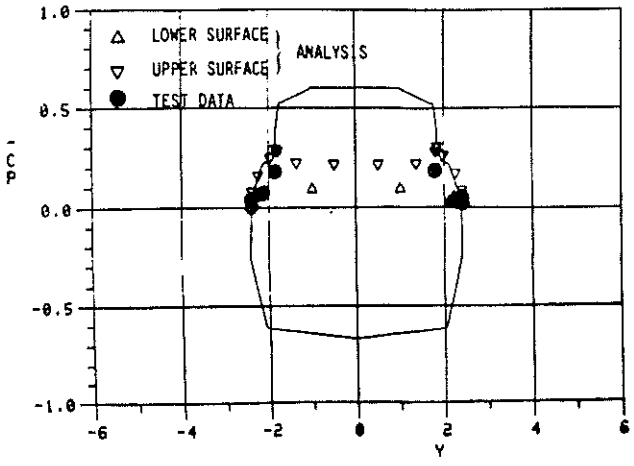

(a) Ref. 4. Run/Point 25/148; Station 17.6 (0.88).

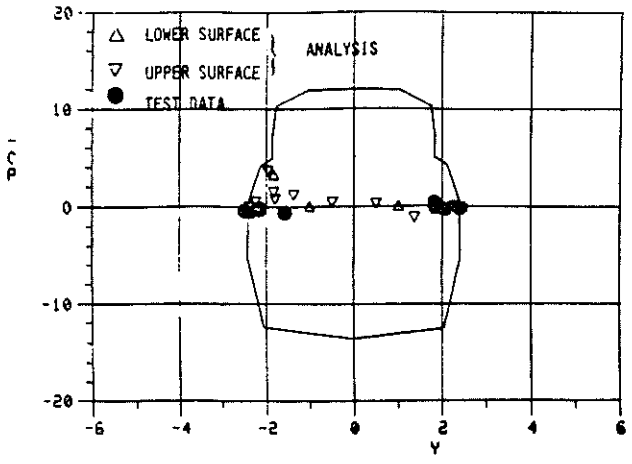

(b) Ref. 4. Run/Point 22/139; Station 17.6 (0.88).

Fig. 7. Correlation with Test Data--0.05 Advance Ratio.

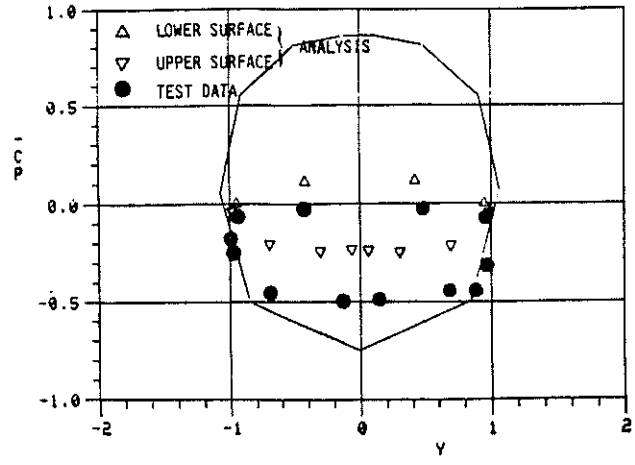

(a) Ref. 4, Run/Point 25/148; Station 1.00 (0.05).

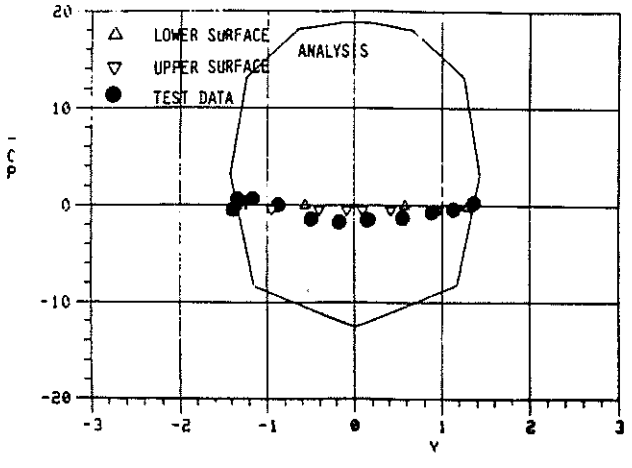

(b) Ref. 4, Run/Point 22/139; Station 1.80 (0.09).

Fig. 8. Correlation with Test Data--0.05 Advance Ratio.

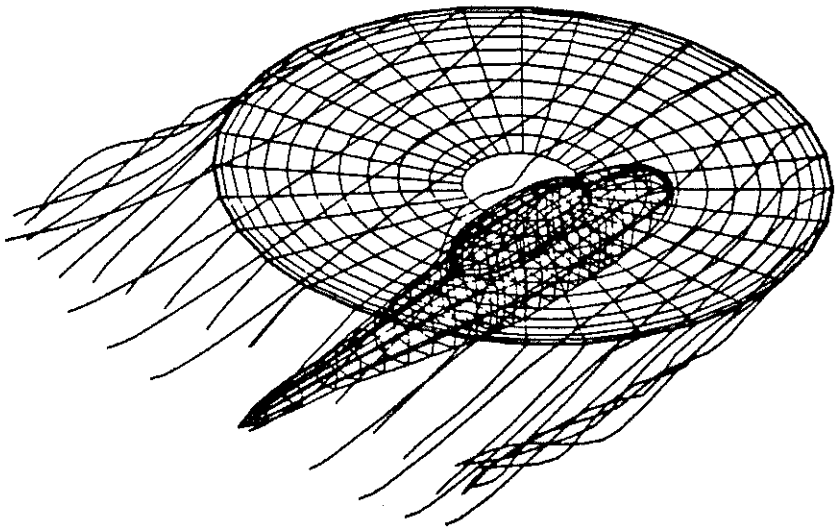

Fig. 9. Calculated Distorted Wake--0.05 Advance Ratio.

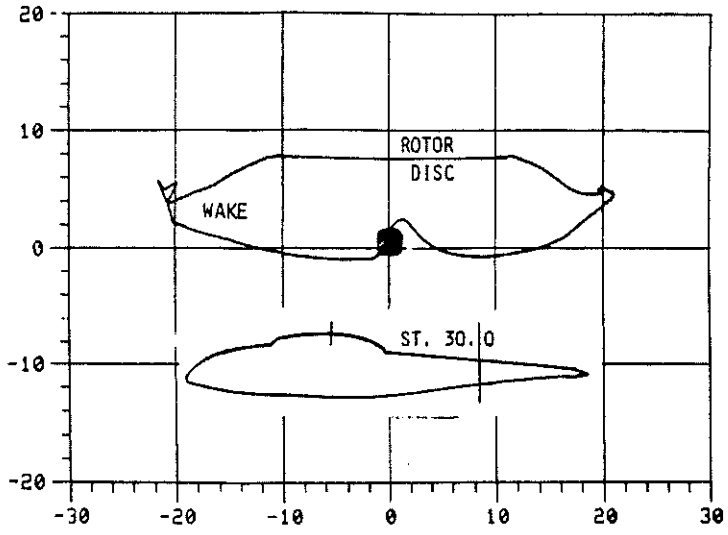

Fig. 10. Calculated Wake Cross Section--0.05 Advance Ratio (Station 30.0).

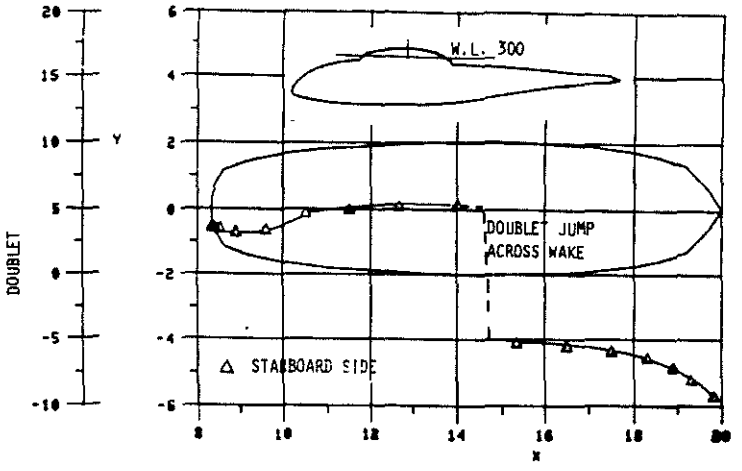

(a) Calculated Pylon Doublet Distribution

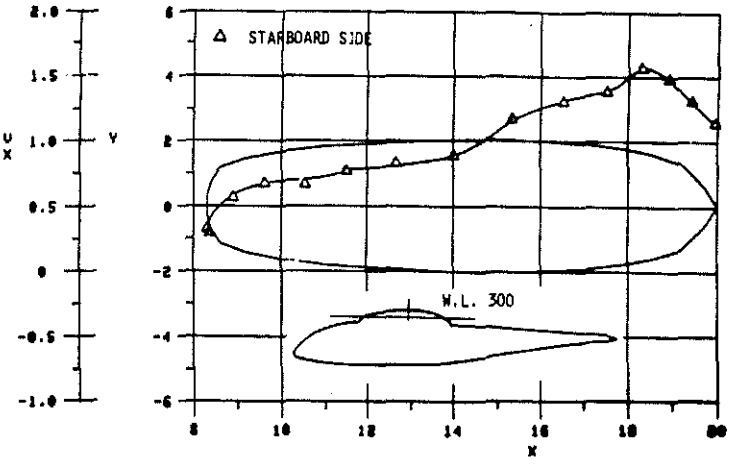

(b) Calculated Pylon Horizontal Velocity Ratio

Fig. 11. Calculated Effect of Wake/Pylon Intersection--0.05 Advance Ratio (Waterline 3.00).

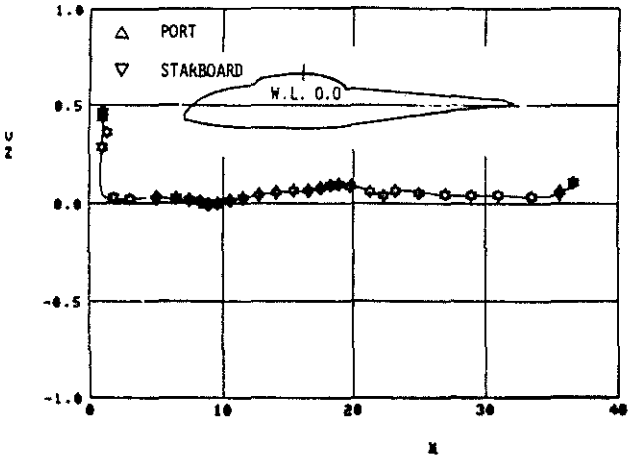

(a) Advance Ratio 0.15

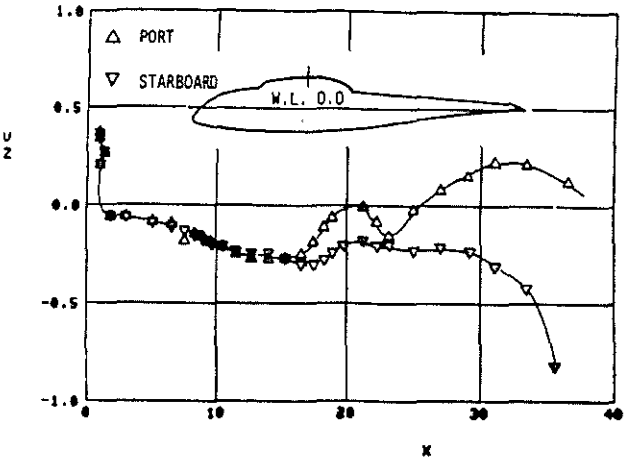

(b) Advance Ratio 0.05

Fig. 12. Calculated Vertical Velocity Ratio, (Waterline 0.0).

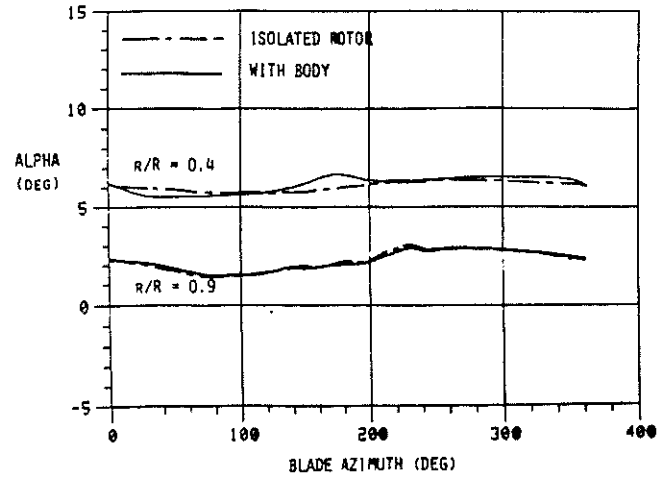

Fig. 13. Calculated Effect of Body on Rotor Angle of Attack--0.05 Advance Ratio.

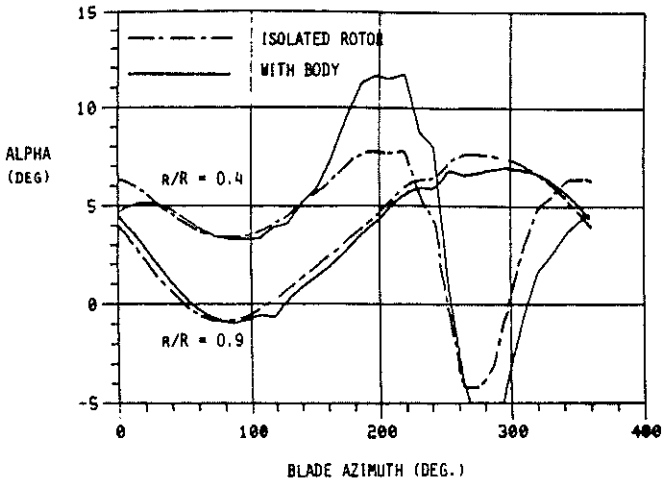

Fig. 14. Calculated Effect of Body on Rotor Angle of Attack--0.30 Advance Ratio.

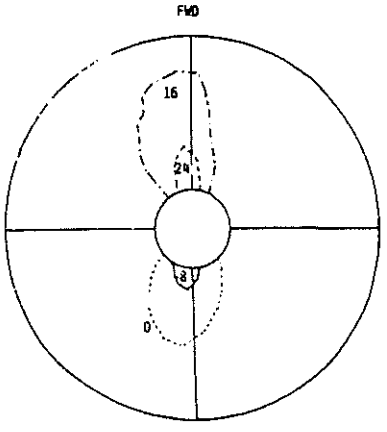

Fig. 15. Calculated Contours of Upwash Velocity in Rotor Plane; Basic Body--0.3 Advance Ratio.

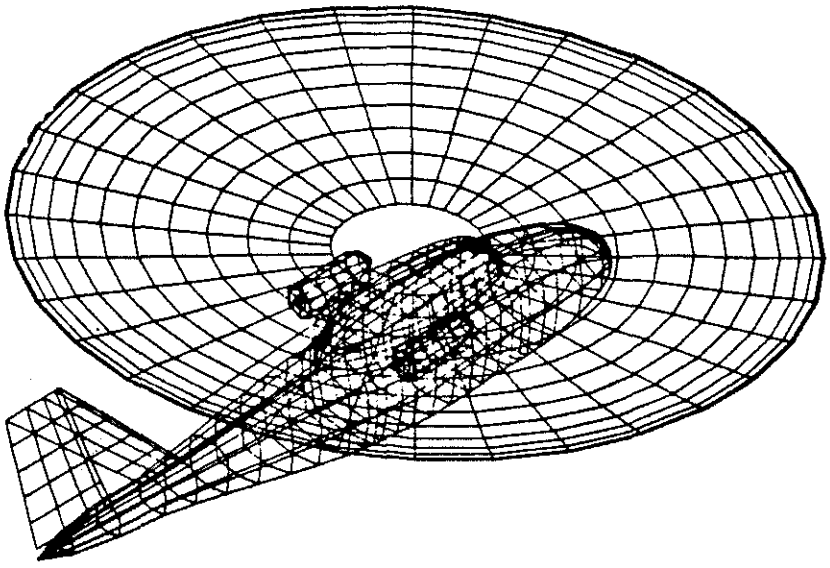

Fig. 16. Basic Body Model with Nacelles and Tail Surfaces Added.

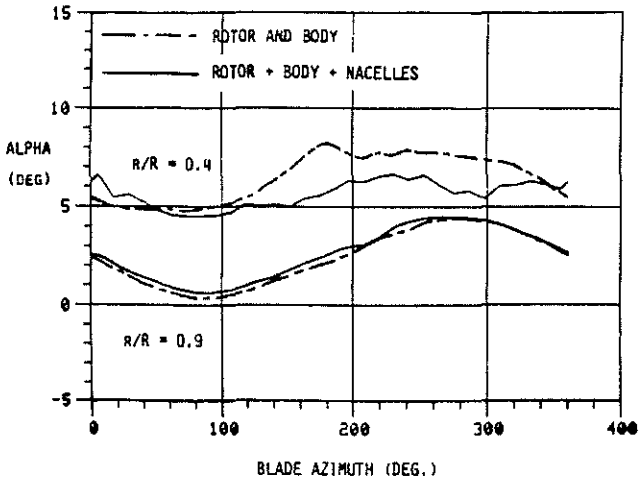

Fig. 17. Effect of Nacelles on Calculated Blade Angle of Attack--0.15 Advance Ratio.

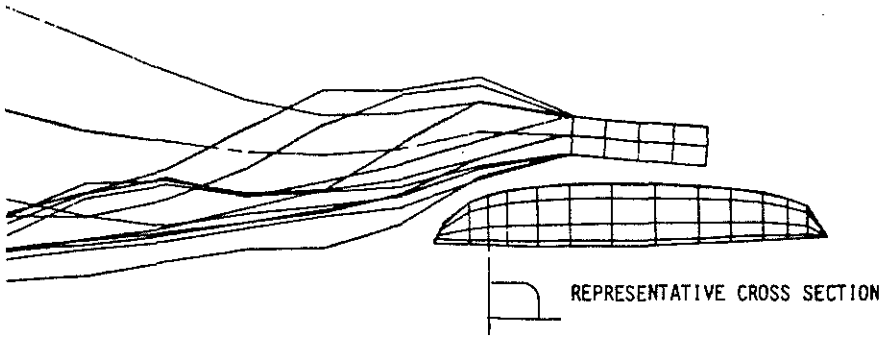

Fig. 18. Calculated Rotor Head Model Wake Development--0.15 Advance Ratio.

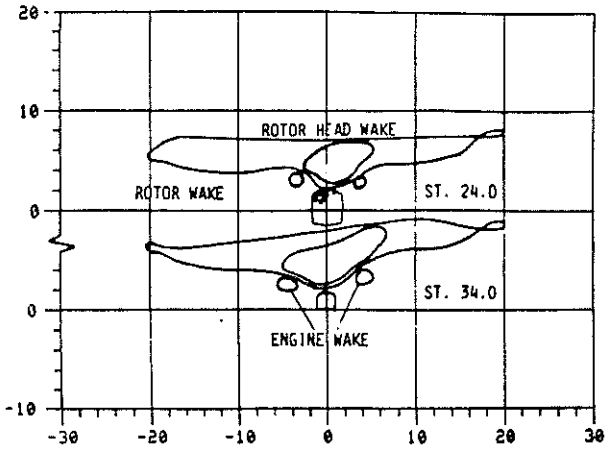

Fig. 19. Rotor Head Wake Cross Sections--0.15 Advance Ratio.

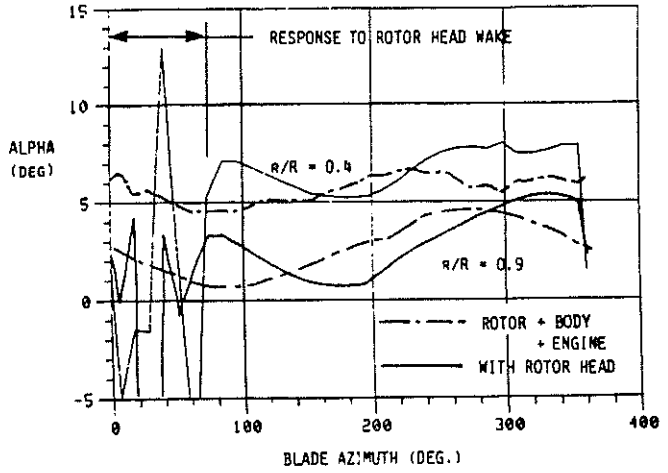

Fig. 20. Effect of Rotor Head on Calculated Blade Angle of Attack--0.15 Advance Ratio.

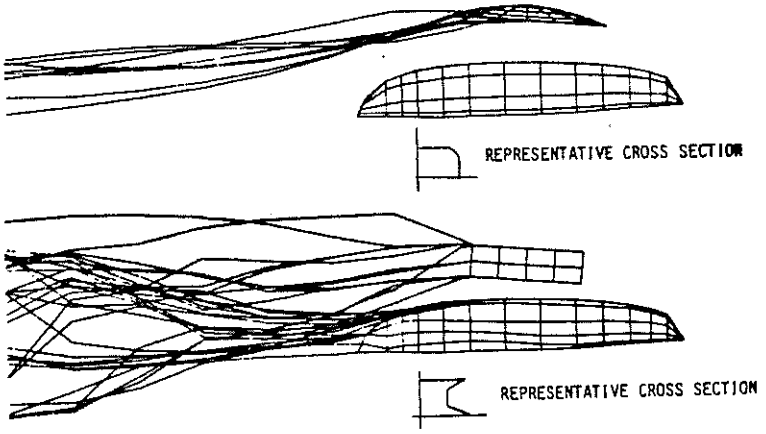

Fig. 21. Calculated Rotor Head Wake Development with Rotor Head Cap and and Modified Pylon--0.15 Advance Ratio.

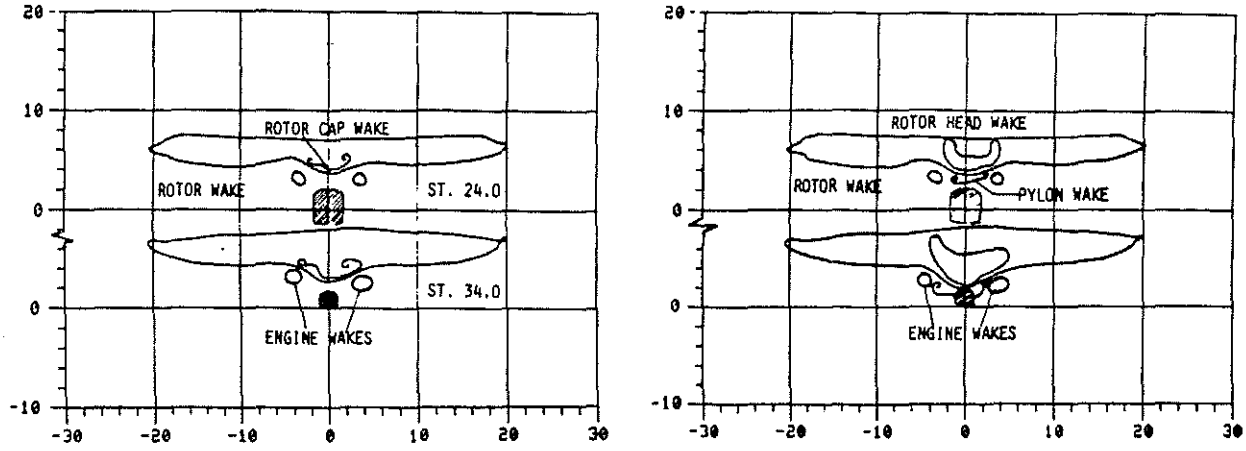

Fig. 22. Calculated Wake Cross Section with Rotor Head Cap and Modified Pylon--0.15 Advance Ratio.

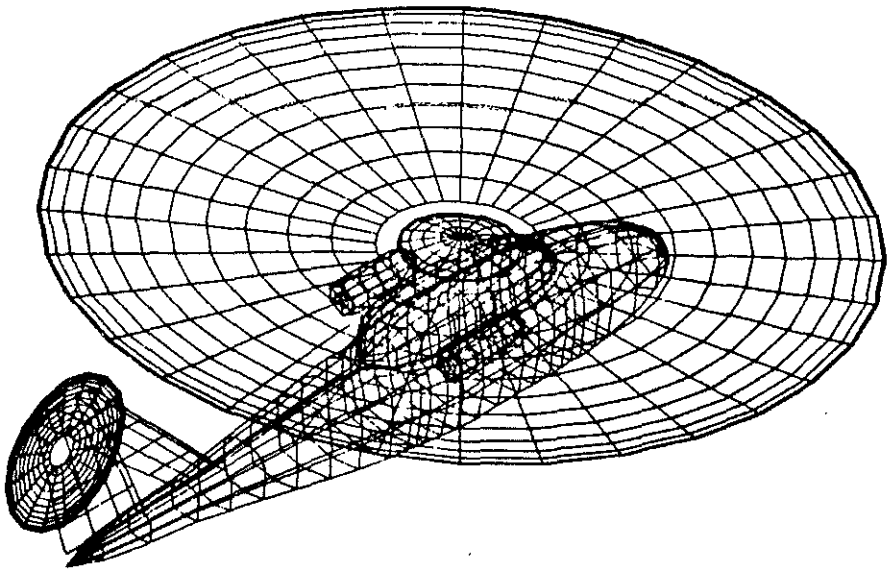

Fig. 23. Full Configuration with Rotor Head Cap.

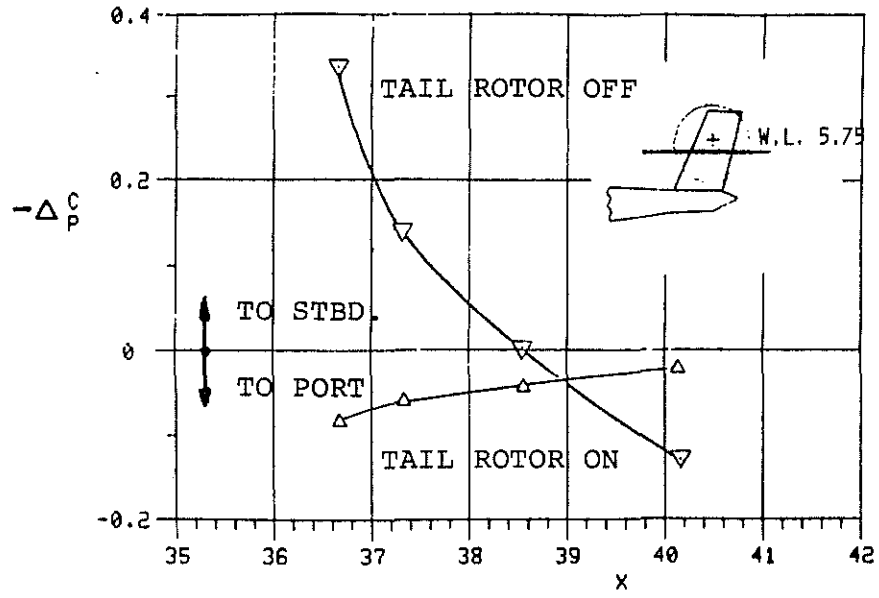

Fig. 24. Effect of Tail Rotor on Vertical Stabiliser Loads (Main Rotor Present--0.15 Advance Ratio).